

# Investigation the catalytic activity of nanofibrillated and nanobacterial cellulose sulfuric acid in synthesis of dihydropyrimidoquinolinetriones

Kobra Nikoofar<sup>1</sup> · Hannaneh Heidari<sup>1</sup> · Yeganeh Shahedi<sup>1</sup>

Received: 5 September 2017 / Accepted: 19 March 2018  
© Springer Science+Business Media B.V., part of Springer Nature 2018

**Abstract** Two novel types of nanocellulose-based catalyst, viz. nanofibrillated cellulose sulfuric acid (s-NFC) and nanobacterial cellulose sulfuric acid (s-BC), were prepared by a simple method and characterized by Fourier-transform infrared spectroscopy, transmission electron microscopy, field-emission scanning electron microscopy, energy-dispersive X-ray spectroscopy, X-ray diffraction analysis, and nitrogen adsorption measurements. The catalytic activity of these two bio-based solid acid catalysts was examined in a one-pot, four-component coupling reaction of barbituric acid, dimedone, aryl aldehydes, and (hetero)aromatic amines in refluxing ethanol. The results confirmed that s-BC promoted the speed of the mentioned reaction more than s-NFC. The recovery and reusability of the degradable nanostructures showed that they could be used in at least three runs without loss of activity.

**Keywords** Nanofibrillated cellulose · Bacterial cellulose · Dihydropyrimidoquinolinetriones · Four-component reaction · Dimedone · Barbituric acid

---

✉ Kobra Nikoofar  
kobranikoofar@yahoo.com; k.nikoofar@alzahra.ac.ir

✉ Hannaneh Heidari  
h.heidari@alzahra.ac.ir; hheidari12@gmail.com

<sup>1</sup> Department of Chemistry, Faculty of Physics and Chemistry, Alzahra University, Vanak, Tehran 1993893973, Iran

## Introduction

Cellulose is one of the most abundant natural biopolymers available on Earth. This biopolymer shows special properties including abundance, nontoxicity, biodegradability, biocompatibility, controlled morphology, and high surface reactivity due to hydroxyl ( $-OH$ ) groups on the surface [1, 2]. These unique properties make it an attractive material for wide applications. Cellulose and its derivatives are considered to be good organic or inorganic supports for catalytic applications [3, 4]. Various studies have reported cellulose sulfuric acid as a recyclable catalyst for various acid-catalyzed reactions [5–8].

On the other hand, within the family of cellulose derivatives, nanocellulose generally covers cellulosic materials in which at least one dimension of the fiber is in the nanoscale range. Nanocellulose offers enhanced properties such as hydrophilicity, high specific surface area, and chemical modifiability using a wide range of reactions [9]. Cellulose nanocrystals and porous cellulose hydrogels can be used as both stabilizers and reducing agents for synthesis of metal catalysts [10–12]. Nanocellulose can be classified into three types of material, viz. nanocrystalline cellulose (NCC), nanofibrillated cellulose (NFC), and bacterial cellulose (BC), produced by acid hydrolysis, mechanical treatment, and bacterial species, respectively [13, 14]. Both NCC and NFC can be isolated from plant-based cellulosic fibers. Compared with NCC, use of NFC is more economical and cost-effective due to its production using mechanical methods. BC is a pure form of cellulose that can be obtained from fermentation of low-molecular-weight sugars, while NC is a composite derived from cellulose and hemicellulose. The high purity and crystalline structure of BC are particularly helpful for improving its properties [9, 15].

Multicomponent reactions (MCRs) are significant tools for versatile preparation of a wide variety of organic and potent medicinal molecules efficiently [16], offering advantages such as environmentally friendliness, atom economy, and avoidance of time-wasting protection–deprotection steps, making them better than multistep organic syntheses. Multifunctionalized heterocycles have attracted special attention due to their multiple and diverse properties. Among this class of compounds, pyrimidine derivatives show biological and medicinal activities such as cancer chemotherapeutic and anti-human immunodeficiency virus (HIV) effects [17, 18]. Pyrimidine fused heterocycles (PFHs) can be found in alkaloids, drugs, antibiotics, agrochemicals, and natural products. Some PFH derivatives are used as antileukemic drugs, potassium-conserving diuretics, and antiallergy drugs. They also possess inflammatory, antioxidant, anticancer, antimicrobial, and antiviral actions [19–21].

A variety of barbituric acid derivatives, a motif of the mentioned dihydropyrimidoquinolinetriones, have been broadly applied as drugs for treatment of cancer and osteoporosis [22]. Dihydroprimido[4,5-*b*]quinolinetriones demonstrate a wide range of activities, including antioxidant [23], antitumor [24], and antiviral effects [25]. In 2011, Khalafi-Nezhad and Panahi prepared this class of compounds via one-pot, four-component reaction of aldehydes, amines, dimedone, and barbituric acid in presence of tungstophosphoric acid ( $H_3PW_{12}O_{40}$ ) in refluxing ethanol [26]. In 2015,

Bhusare et al. used [Msim]Cl ionic liquid to catalyze this four-component condensation to afford the desired products [27]. Their initial assays indicated good inhibition activity of some derivatives against the human breast cancer cell line MCF7. Based on our search results, no other papers describing preparation of this class of compounds have been published. According to the unique properties of nanocellulose and the worthwhile properties and applications of dihydropyrimidoquinolinetrienes, we prepared two novel kinds of sulfuric acid-embedded nanocellulose, viz. nanofibrillated cellulose sulfuric acid (s-NFC) and bacterial nanocellulose sulfuric acid (s-BC), for the first time. These two nanostructures were characterized by Fourier-transform infrared (FTIR) spectroscopy, transmission electron microscopy (TEM), field-emission scanning electron microscopy (FE-SEM), and energy-dispersive X-ray spectroscopy (EDS) analysis. Their catalytic activity was examined in preparation of dihydropyrimidoquinolinetrienes through one-pot, four-component reactions of substituted benzaldehydes, aniline derivatives, dimedone, and barbituric acid in refluxing ethanol. It must be mentioned that, in 2016, Sadeghi and Sowlat Tafti reported nanocrystalline cellulose (NCC) sulfuric acid as catalyst for synthesis of pyrano[4,3-*b*]pyrans [28]. Presence of sulfuric acid as a functional group on the surface of nanocellulose increases the surface polarity and acidity and thereby the catalytic efficiency of nanocellulose-OSO<sub>3</sub>H [29].

## Experimental

### Materials and instrumentation

All chemicals were purchased from Merck, Aldrich, and Alfa Aesar chemical companies and were used without further purification. Commercial-grade cellulose nanofibers (NFC and BC) were supplied from Nano Novin Polymer Co., Iran. NFC is produced from lignocellulosic sources such as wood and agricultural residues by mechanical force (grinding), i.e., a top-down mechanism. BC hydrogel is produced via a bottom-up approach by some bacteria species, especially *Acetobacter xylinum* in aqueous culture [29, 30].

The morphology of the samples was analyzed using a Tescan Mira2 field-emission scanning electron microscope. The samples were coated with gold using a vacuum sputter-coater. EDS analysis was carried out using a SAMx-analyzer. TEM images were taken with Philips model MC30 and Zeiss model EM10C instruments. IR spectra were recorded from KBr disk using an FT-IR Bruker Tensor 27 instrument. Melting points were determined on an Electrothermal 9200 analyzer and are uncorrected. X-ray diffraction patterns were obtained using a Philips PW1730 X-ray diffractometer with Cu K<sub>α</sub> radiation at 40 kV and 30 mA. Samples were scanned in the  $2\theta$  range between 10° and 80°. <sup>1</sup>H and <sup>13</sup>C nuclear magnetic resonance (NMR) spectra were recorded using a Bruker DRX (400 MHz) device. Reaction progress was monitored by thin-layer chromatography (TLC) using commercially available silica gel sheets. Preparative layer chromatography (PLC) was carried out on 20 × 20 cm<sup>2</sup> plates, coated with a 1-mm-thick layer of Merck silica gel PF<sub>254</sub>, prepared by applying the silica as slurry and drying in air. The

products were characterized by comparison of their melting point as well as spectroscopic data (FT-IR,  $^1\text{H}$  and  $^{13}\text{C}$  NMR).

### Preparation of nanofibrillated cellulose sulfuric acid (s-NFC) and nanobacterial cellulose sulfuric acid (s-BC)

Both nanocellulose sulfuric acids (s-NFC and s-BC) were prepared according to previous studies with slight modification [28]. A volume of 0.4 mL chlorosulfonic acid was added dropwise to well-stirred slurry containing 1.00 g of each nanocellulose source (NFC or BC) in *n*-hexane at 0 °C during 20 min. After completion of the addition, the mixture was stirred for 2 h at room temperature to remove HCl from the reaction vessel. Then the mixture was filtered, and the collected solid washed with methanol (30 mL) and air-dried at room temperature to obtain s-NFC and s-BC nanostructures as tough black solids.

### General procedure for synthesis of dihydropyrimidoquinolinetrienes catalyzed by s-NFC and s-BC

A mixture of aldehydes (**1a–h**, 1 mmol), amines (**2a–g**, 1 mmol), dimedone (**3**, 1 mmol), barbituric acid (**4**, 1 mmol), and s-NFC or s-BC (0.024 g) in refluxing ethanol (5 mL) was stirred for appropriate reaction time monitored by TLC (*n*-hexane/EtOAc eluent, 3:2). After reaction completion, methanol (5 mL) was added, followed by filtering. The solid residue was washed with further methanol (2 × 5 mL). Product purification was achieved by plate chromatography to give corresponding solid products **5a–j** in high yield.

#### *5,10-Bis(4-hydroxyphenyl)-8,8-dimethyl-8,9-dihydropyrimido[4,5-*b*]quinoline-2,4,6(1*H*,3*H*,5*H*,7*H*,10*H*)-tri-one (5d)*

Black solid. M.p. 166–169 °C; IR (KBr,  $\text{cm}^{-1}$ )  $\nu$ : 3419, 1739, 1650, 1485, 1239;  $^1\text{H}$  NMR (DMSO- $d_6$ , 400 MHz) ( $\delta$ , ppm): 3.72 (s, 3H,  $-\text{OCH}_3$ ), 6.99–8.4 (m,  $-\text{ArH}$ ), 10.92 (s, 1H, NH), 11.69 (s, 1H, NH);  $^{13}\text{C}$  NMR ( $\delta$ ): 27.4, 33.3, 52.5, 84.5, 112.4, 118.4, 120.1, 125.3, 125.5, 126.2, 127.6, 127.7, 128.6, 129.4, 130.5, 150.5, 151.2, 160.5, 162.3. GC-mass:  $m/z$  378 ( $[\text{M}^+-2]\text{Me}$ ), 314 ( $\text{M}^+-\text{CH}_2\text{CHCO}_2\text{Me}$ ), 302 ( $[\text{M}^+]$ -aniline), 284 ( $[\text{M}^+]-\text{CO}_2$ ,  $-\text{NHCOEt}$ ), 270 ( $[\text{M}^+]-\text{C}_6\text{H}_5\text{NO}_2$ ).

#### *5-(4-Hydroxy-3-methoxyphenyl)-10-(2-nitrophenyl)-8,8-dimethyl-8,9-dihydropyrimido[4,5-*b*]quinoline-2,4,6(1*H*,3*H*,5*H*,7*H*,10*H*)-trione (5e)*

Orange solid. M.p. 180–182 °C; IR (KBr,  $\text{cm}^{-1}$ )  $\nu$ : 3400, 1710, 1671, 1595, 1464, 1362, 1271;  $^1\text{H}$  NMR (DMSO- $d_6$ , 400 MHz) ( $\delta$ , ppm): 2.23 (s, 3H,  $-\text{CH}_3$ ), 3.56 (s, 3H,  $-\text{OCH}_3$ ), 6.61–7.96 (m,  $-\text{ArH}$ ), 9.99 (s, 1H, NH), 10.33 (s, 1H, NH);  $^{13}\text{C}$  NMR ( $\delta$ ): 27.4, 33.3, 52.5, 84.5, 112.4, 118.4, 120.1, 125.3, 125.5, 126.2, 127.6, 127.7, 128.6, 129.4, 130.5, 150.5, 151.2, 160.5, 162.3. GC-mass:  $m/z$  378 ( $[\text{M}^+-2]\text{-Me}$ ), 314 ( $\text{M}^+-\text{CH}_2\text{CHCO}_2\text{Me}$ ), 302 ( $[\text{M}^+]$ -aniline), 284 ( $[\text{M}^+]-\text{CO}_2$ ,  $-\text{NHCOEt}$ ), 270 ( $[\text{M}^+]-\text{C}_6\text{H}_5\text{NO}_2$ ).

5-(1*H*-Pyrrol-2-yl)-10-(1*H*-5-methylpyrazol-3-yl)-8,8-dimethyl-8,9-dihydropyrimido[4,5-*b*]quinoline-2,4,6(1*H*,3*H*,5*H*,7*H*,10*H*)-trione (**5i**)

Black solid. M.p. 243–246 °C; IR (KBr,  $\text{cm}^{-1}$ )  $\nu$ : 3419, 1730, 1610, 1576, 1408, 1268;  $^1\text{H}$  NMR (DMSO- $d_6$ , 400 MHz) ( $\delta$ , ppm): 3.15 (s, 3H,  $-\text{OCH}_3$ ), 6.93–8.57 (m,  $-\text{ArH}$ ), 9.16 (s, 1H, NH), 10.47 (s, 1H, NH), 10.94 (s, 1H, NH);  $^{13}\text{C}$  NMR ( $\delta$ ): 27.4, 33.3, 52.5, 84.5, 112.4, 118.4, 120.1, 125.3, 125.5, 126.2, 127.6, 127.7, 128.6, 129.4, 130.5, 150.5, 151.2, 160.5, 162.3. GC-mass:  $m/z$  378 ( $[\text{M}^+-2]-\text{Me}$ ), 314 ( $[\text{M}^+-\text{CH}_2\text{CHCO}_2\text{Me}]$ ), 302 ( $[\text{M}^+]-\text{aniline}$ ), 284 ( $[\text{M}^+]-\text{CO}_2$ ,  $-\text{NHCOEt}$ ), 270 ( $[\text{M}^+]-\text{C}_6\text{H}_5\text{NO}_2$ ).

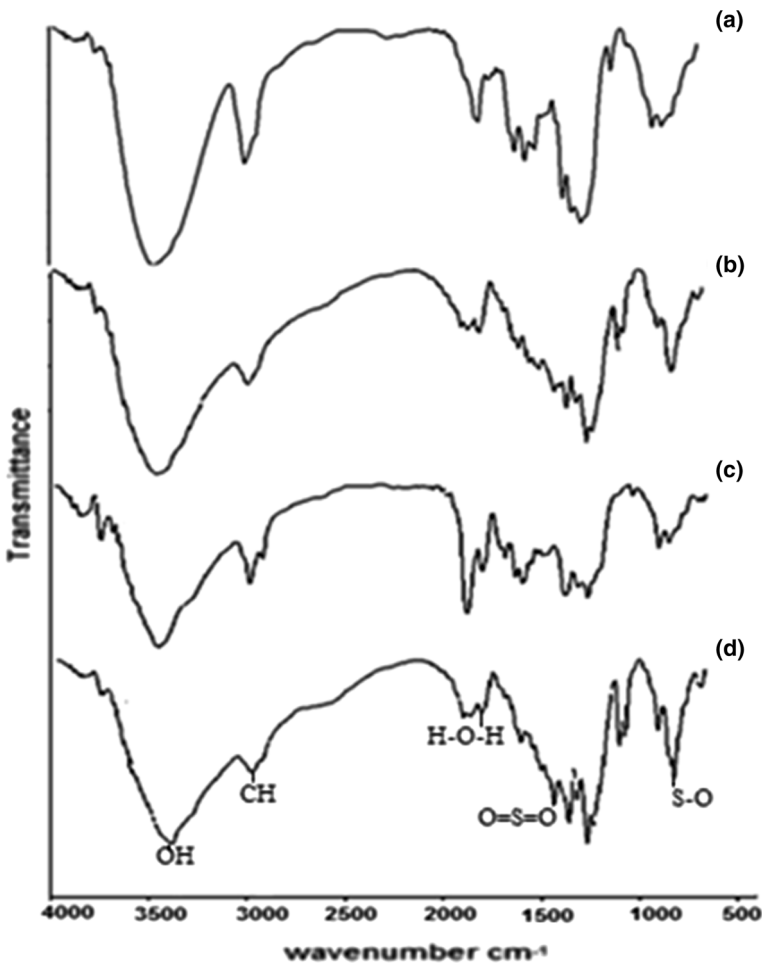


**Fig. 1** FT-IR spectrum of (a) NFC, (b) s-NFC, (c) BC, and (d) s-BC

## Results and discussion

### Characterization of s-NFC and s-BC

Consistent structure of the catalysts was found by FTIR, TEM, FE-SEM, and EDS. The FTIR spectra of nanocellulose and nanocellulose sulfuric acid are shown in Fig. 1, revealing dominant peaks at approximately  $3300\text{--}3400$  and  $2900\text{ cm}^{-1}$ , corresponding to stretching vibrations of OH and CH groups, respectively. Other peaks such as those at  $1635\text{ cm}^{-1}$  (H–O–H bending vibration) were also observed in the spectra. For s-NFC and s-BC, three peaks at  $1010\text{--}1100$ ,  $1200\text{--}1250$ , and  $650\text{ cm}^{-1}$  were related to symmetric, and asymmetric O=S=O and S–O stretching vibration peaks, respectively [31]. The OH vibration in nanocellulose sulfuric acid was broader due to overlap between OH vibrations of sulfonic group with the OH vibration of cellulose.

The morphology and size of the two different forms of nanocellulose (NFC and BC) and sulfonated nanocelluloses were studied using FE-SEM. For NFC, fibrous

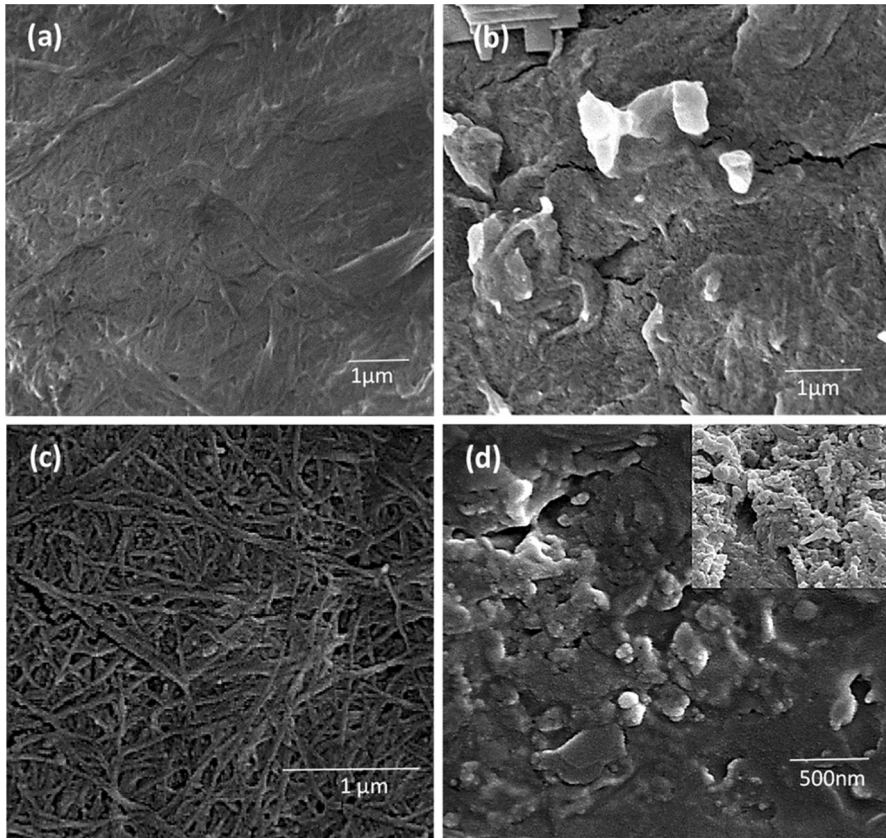


**Fig. 2** FE-SEM of **a** nanofibrillated cellulose (NFC), **b** nanocellulose sulfuric acid (s-NFC), **c** bacterial cellulose (BC), and **d** bacterial cellulose sulfuric acid (s-BC)

network structure and fibril aggregates were observed (Fig. 2a). In contrast to NFC, BC possessed individualized, more uniform and slender nanofibers (Fig. 2c). In s-NFC, brighter aggregates appearing on the darker surface are bumps produced by sulfonic acid modification (Fig. 2b), however EDS spot analysis showed higher amount of sulfur in these spots. s-BC showed a more disperse structure on the surface with higher content of sulfur (Fig. 2d).

Figure 2d also shows that the porosity of bacterial cellulose was reduced after sulfonic acid modification. Nitrogen adsorption measurements also indicated that incorporation of sulfonic acid groups in the nanocellulose structure decreased the pore diameter, Brunauer–Emmett–Teller (BET) surface area, and pore volume compared with native nanocellulose. The structural parameters for neat BC and s-BC are presented in Table 1. The decrease in the surface area of s-BC could be due to reaction of the surface sites with chlorosulfonic acid, causing the surface to become crowded with  $\text{OSO}_3\text{H}$  and thus blocking pores, as reported by Hello et al. [32].

As seen in Fig. 3, EDS analysis revealed C and O as the main elements present in the nanocellulose. The spectrum obtained for sulfonated nanocellulose indicated presence of sulfur on the surface. The sulfur loading on NFC and BC measured by EDS analysis was 7.97 and 11.06 wt%, respectively.

TEM images of the nanostructures were taken to examine the structural shape and size of the nanofibers. The NFC scaffold appeared as twisted and entangled nanofibers on TEM (Fig. 4a). The dimension of a single nanocellulose fiber could be measured as  $\sim 100$  nm (Fig. 4b). TEM of BC showed individual fibrils with width of approximately 10 nm and length of several micrometers (Fig. 4c, d).

The crystalline structure of NFC and BC was determined by X-ray diffraction (XRD) analysis (Fig. 5). In this study, NFC exhibited characteristic peaks related to cellulose lattice planes located at  $2\theta = 15.76^\circ$  (101),  $22.65^\circ$  (002), and  $34.4^\circ$  (040) (Fig. 5a). The diffraction pattern of BC showed the typical diffraction peaks of native cellulose at  $14.3^\circ$ ,  $16.8^\circ$ ,  $22.5^\circ$ , and  $34.4^\circ$ , corresponding to diffraction from 101, 101, 002, and 040 planes, respectively (Fig. 5b). In NFC, as compared with BC, the presence of a single peak at  $15.76^\circ$  instead of two distinct peaks at  $2\theta = 14.3^\circ$  and  $16.8^\circ$  can be related to presence of noncellulosic compounds such as hemicellulose and the difference in the cellulose crystal structure of NFC [33]. These XRD results indicate presence of hemicellulose in NFC and high purity and crystalline structure for BC.

**Table 1** BET surface area, pore volume, and pore diameter of BC and s-BC

Entry	Sample	$S_{\text{BET}}$ ( $\text{m}^2 \text{g}^{-1}$ )	Total pore volume ( $\text{cm}^3 \text{g}^{-1}$ )	Mean pore diameter (nm)
1	BC	4.332	0.011613	10.723
2	s-BC	0.71526	0.0016955	9.482

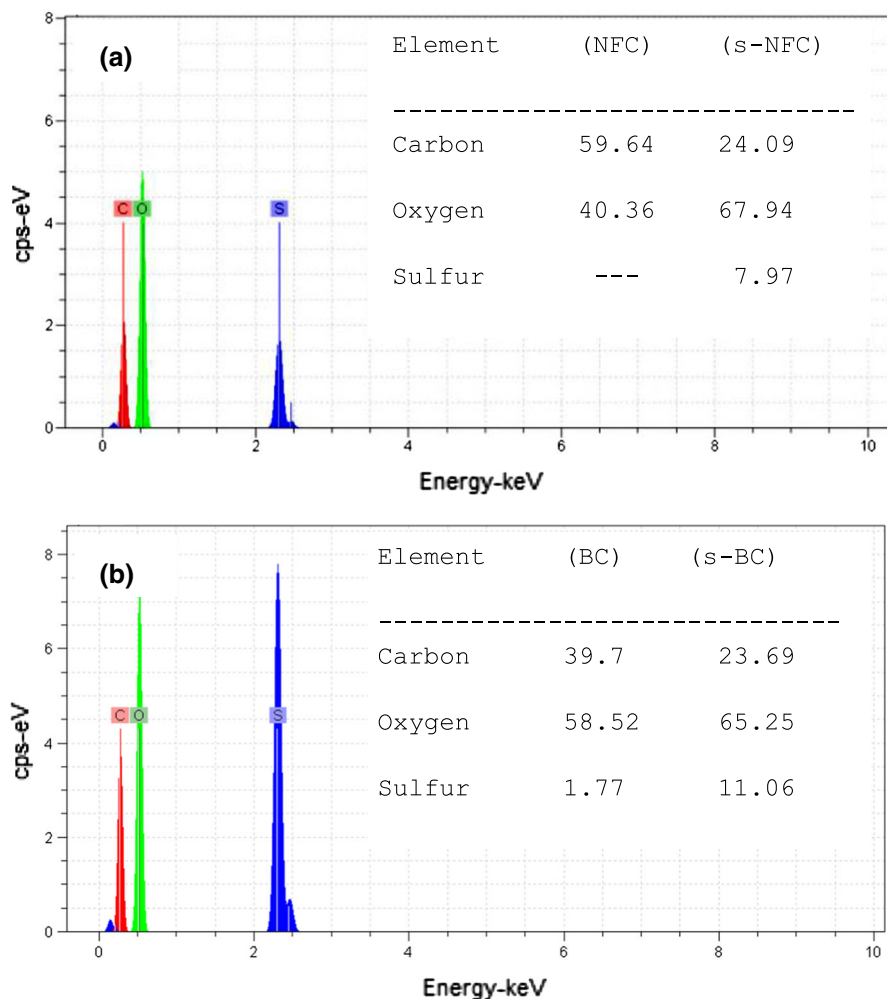


**Fig. 3** EDS of **a** s-NFC and **b** s-BC

### Catalytic activity of s-NFC and s-BC in synthesis of dihydropyrimidoquinolinetriones

The catalytic activity of the prepared cellulosic-based nanostructures was investigated in preparation of dihydropyrimido[4,5-*b*]quinolinetriones. To optimize the reaction conditions, the one-pot, one-step reaction of *N,N*-dimethylbenzaldehyde (**1b**, 1 mmol), 4-methoxyaniline (**2d**, 1 mmol), dimedone (**3**, 1 mmol), and barbituric acid (**4**, 1 mmol) was first considered as model reaction to determine the effect of various parameters (Table 2). The results showed that, in absence of solvent, the reaction proceeded smoothly (Table 2, entries 1, 2). The model reaction progressed in presence of H<sub>2</sub>O or ethanol solvent at room temperature and also under reflux condition. The best results were obtained in refluxing ethanol

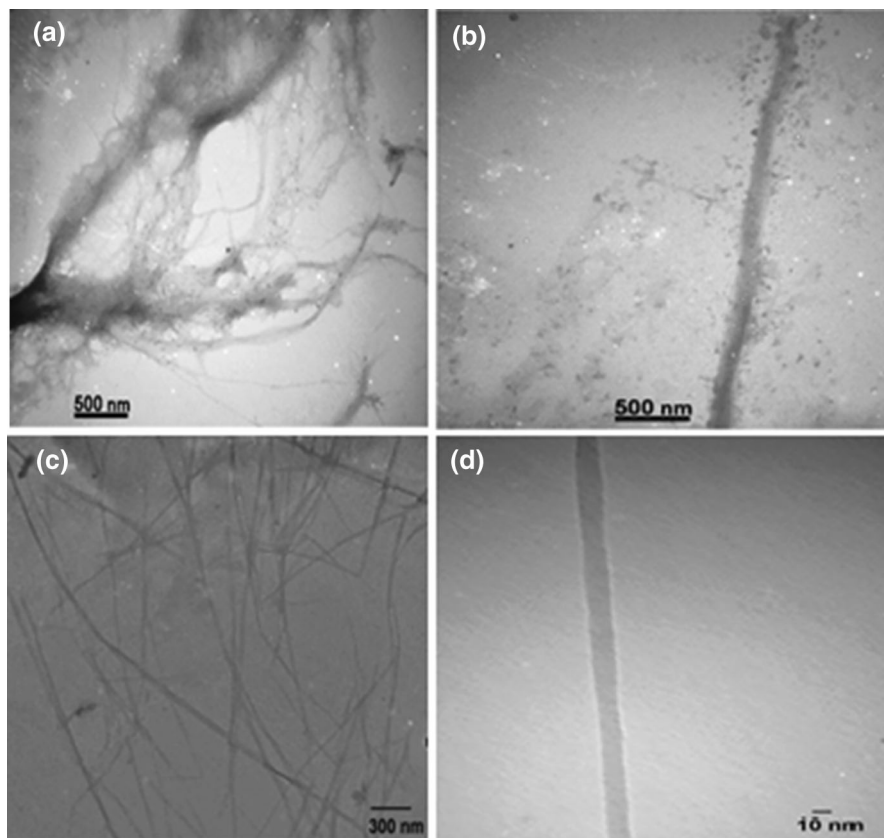


**Fig. 4** TEM images of **a** NFC and **b** zoomed view on a single NFC fiber, **c** BC, and **d** zoomed view on a single BC fiber

(entries 3–6). It seems that elevating the temperature affected the reaction progress. Investigation of the amount of s-NFC catalyst revealed 0.024 g as the best amount (Table 2, entries 6–8). The condensation was also carried out in catalyst-free conditions, but the desired product was not successfully achieved (entry 9). These results confirm the promoting effect of s-NFC in preparation of 8,9-dihydro-8,8-dimethyl-5-(4-*N,N*-dimethyldiphenyl)-10-(4-methoxydiphenyl)pyrimido[4,5-*b*]quinolone-2,4,6(1*H*,3*H*,5*H*,7*H*,10*H*)-trione (**5b**). All experiments occurred in one-pot, one-step mode.

Based on the optimized condition, the reaction of aldehydes (**1a–h**), amines (**2a–g**), dimedone (**3**), and barbituric acid (**4**) proceeded in presence of s-NFC (0.024 g) in refluxing ethanol (Scheme 1). The results are summarized in column A of Table 3, showing that benzaldehyde (**1a**) and its electron-donating as well as electron-withdrawing derivatives underwent the four-component condensation with aniline (**2a**) well (entries 1–5, column A). Indole-3-carbaldehyde (**1f**), as a hindered heteroaromatic aldehyde, was also examined for this condensation, with good results (entries 6, 7). To show the wide range of efficacy of the procedure,

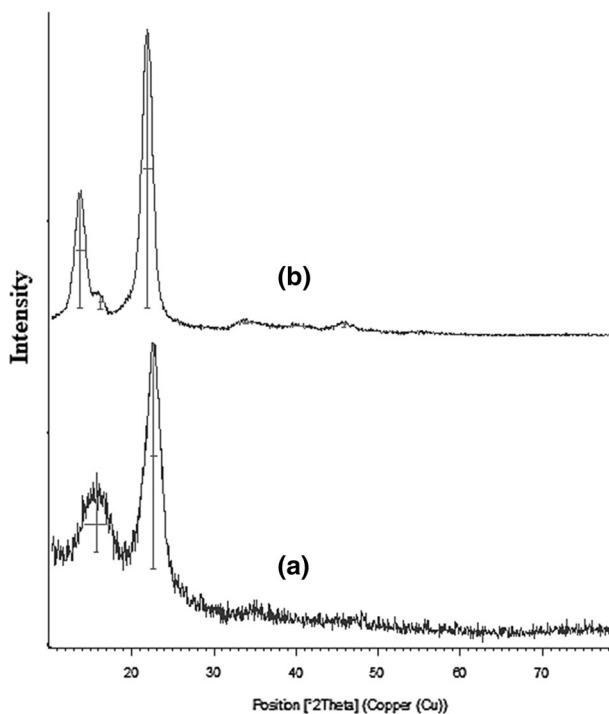


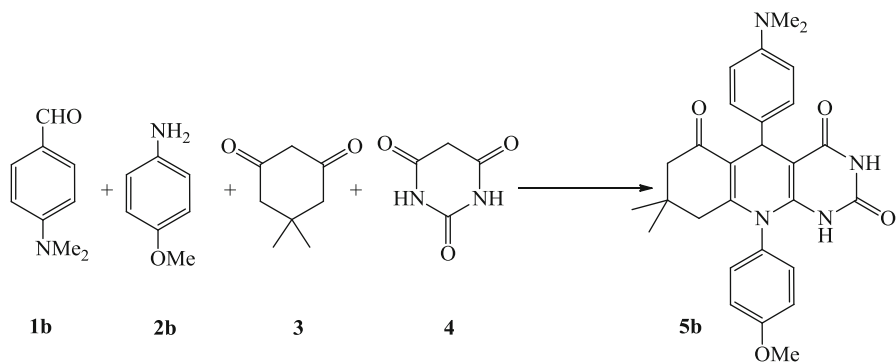
**Fig. 5** XRD patterns of (a) NFC and (b) BC

ammonium acetate (**2f**) was also utilized as amine source to obtain the corresponding product **5h** successfully (entry 8). Use of pyrrole-2-carbaldehyde (**1g**) and 3-amino-1,2,4-triazole (**2g**), as a potent pharmaceutically heteroaromatic amine, resulted in the interesting molecule **5i** in good yield (entry 9). The selectivity of the protocol was also examined using terephthalaldehyde (**1h**) with 4-methoxyaniline (**2c**). The corresponding product of condensation was observed at both aldehydic functional groups (entry 10). We also changed the amount of catalyst from 0.048 to 0.024 g, but no byproduct, related to condensation of one aldehyde position of terephthalaldehyde, was observed.

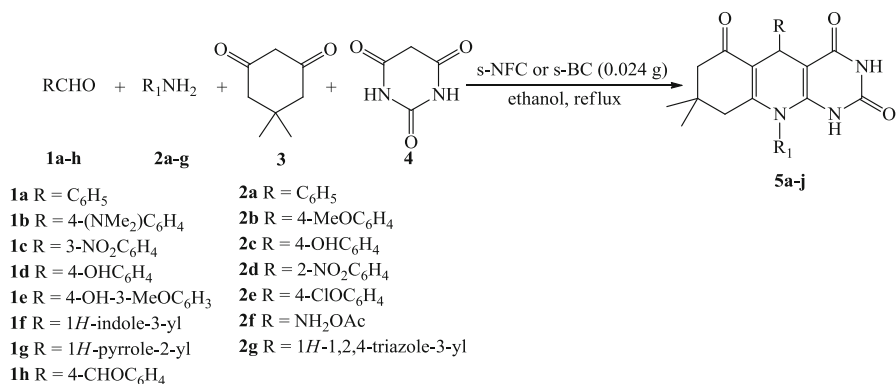
In the next step, the catalytic activity of the other prepared nanocatalyst s-BC was examined to obtain the desired dihydropyrimido[4,5-*b*]quinolinetrione derivatives. The results are presented in column B of Table 3. As seen, use of s-BC shortened the reaction times. According to these results and the BET and SEM results for sulfonated nanocellulose (Table 1, Fig. 2c, d), increasing the catalytic activity of the s-BC sample, despite the porosity reduction, represents the dominant effect of the sulfonic acid substitution.

All products were isolated and characterized by their melting point and spectroscopic data (FT-IR,  $^1\text{H}$  NMR,  $^{13}\text{C}$  NMR, and mass) in comparison with authentic samples.

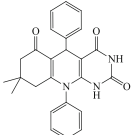
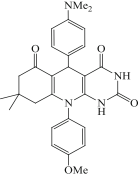
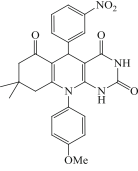
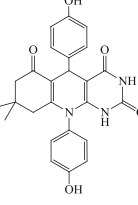
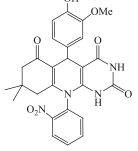
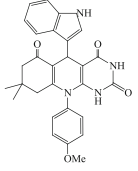
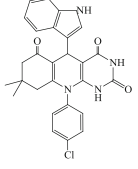
Finally, the reusability and recovery of the synthesized biobased nanocatalyst was investigated in preparation of 8,8-dimethyl-5,10-diphenyl-8,9-

**Table 2** Investigation of reaction conditions for synthesis of **5b**

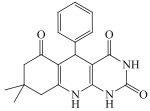
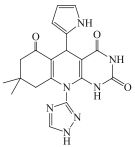
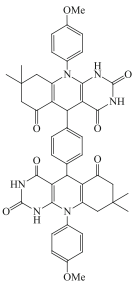
Entry	s-NFC amount (g)/solvent (5 mL)/temp. (°C)	Time (min)	Yield (%) <sup>a</sup>
1	0.024/-/rt	300	18
2	0.024/-/70	240	5
3	0.024/H <sub>2</sub> O/rt	210	35
4	0.024/H <sub>2</sub> O/reflux	120	55
5	0.024/EtOH/rt	130	60
6	0.024/EtOH/reflux	90	90
7	0.016/EtOH/reflux	170	75
8	0.04/EtOH/reflux	150	85
9	-/EtOH/reflux	400	8

<sup>a</sup> Isolated yield**Scheme 1** Synthesis of dihydropyrimido[4,5-*b*]quinolinetriones using s-NFC or s-BC

**Table 3** Synthesis of dihydropyrimido[4,5-*b*]quinolinetriones in the presence of s-NFC (column A) and s-BC (column B) in refluxing ethanol<sup>a</sup>

Entry	Product	A		B		Mp (°C) <sup>b</sup>	
		Time (min)	Yield (%)	Time (min)	Yield (%)		
1		<b>5a</b>	45	92, 90, 90 <sup>c</sup>	40	94	231–233 [26]
2		<b>5b</b>	90	90	70	91	263–264 [26]
3		<b>5c</b>	60	85	50	83	256–257 [26]
4		<b>5d</b>	105	95	90	94	166–169 new
5		<b>5e</b>	90	93	80	90	180–182 new
6		<b>5f</b>	165	93	150	91	252–254 [26]
7		<b>5g</b>	105	95	95	90	275–277 [26]

**Table 3** continued

Entry	Product	A		B		Mp (°C) <sup>b</sup>	
		Time (min)	Yield (%)	Time (min)	Yield (%)		
8		<b>5h</b>	75	90	60	88	208–210 [26]
9		<b>5i</b>	75	90	65	88	243–246 New
10 <sup>d</sup>		<b>5j</b>	90	55	80	54	301–303 [26]

<sup>a</sup>Amine (1 mmol), aldehyde (1 mmol), dimedone (1 mmol), and barbituric acid (1 mmol) in presence of 0.024 g of s-NFC (column A) or s-BC (column B)

<sup>b</sup>Reference of known compounds

<sup>c</sup>Results for recovery and reusability of catalyst

<sup>d</sup>**1h:2b:3:4** at molar ratio of 1:2:2:2 in presence of 0.048 g of each catalyst

dihydropyrimido[4,5-*b*]quinoline-2,4,6(1*H*,3*H*,5*H*,7*H*,10*H*)-trione (**5a**). After reaction completion, ethanol (10 mL) was added to the reaction mixture, and the catalyst was filtered and washed with further ethanol (2 × 5 mL). After evaporation of the solvent followed by air drying, the solid residue was utilized in another run. The results in Table 3 (column A, entry 1) show that the catalyst could be recovered and reused simply in at least three runs without loss of activity, in agreement with green catalytic reaction principles.

## Conclusions

We developed a convenient, efficient, and ecofriendly protocol for synthesis of dihydropyrimido[4,5-*b*]quinolinetriones through one-pot one-step four-component reaction of dimedone, barbituric acid, benzaldehydes, and amines in refluxing ethanol in presence of two newly synthesized kinds of nanocellulose sulfuric acid,

viz. s-NFC and s-BC. We found that sulfonation played a more important role in their catalytic activity in comparison with porosity. The procedure offers several advantages, including mild and neutral condition, good product yield, short reaction time, operational simplicity, minimum environmental impact, and easy workup. The catalysts are also biodegradable and reusable, in agreement with green chemistry principles.

**Acknowledgements** The researchers greatly appreciate the Research of Alzahra University for their financial support of this study.

## References

1. W. Chen, H. Yu, Y. Liu, P. Chen, M. Zhang, Y. Hai, *Carbohydr. Polym.* **83**, 1804 (2011)
2. S.Y. Lee, D.J. Mohan, I.A. Kang, G.H. Doh, S. Lee, S.O. Han, *Fiber. Polym.* **10**, 77 (2009)
3. A. Rahmatpour, *React. Funct. Polym.* **71**, 80 (2011)
4. N.Y. Baran, T. Baran, A. Mendes, *Appl. Catal. A-Gen.* **531**, 36 (2017)
5. R.H. Vekariya, H.D. Patel, *ARKIVOC* **1**, 136 (2015)
6. A. Zonouzi, Z. Izakian, K. Abdi, S.W. Ng, *Helv. Chim. Acta* **99**, 355 (2016)
7. S. Maddila, M. Momin, P. Lavanya, C.V. Rao, *J. Saudi Chem. Soc.* **20**, 173 (2016)
8. S.M. Gomha, S.M. Riyadh, *J. Braz. Chem. Soc.* **26**, 916 (2015)
9. K.Y. Lee, T. Tammelin, K. Schulfter, H. Kiiskinen, J. Samela, A. Bismarck, *ACS Appl. Mater. Interfaces* **4**, 4078 (2012)
10. C. Wu, W. Lu, G. Zhang, R. Yuan, X. Xiong, J. Zhang, *Mater. Chem. A* **1**, 8645 (2013)
11. X. Wu, C. Lu, Z. Zhou, G. Yuan, R. Xiong, X. Zhang, *Environ. Sci. NANO* **1**, 71 (2014)
12. Y. Han, X. Wu, X. Zhang, Z. Zhou, C. Lu, *ACS Sustain. Chem. Eng.* **4**, 6322 (2016)
13. M.V.G. Zimmermann, C. Borsoi, A. Lavoratti, M. Zanini, A.J. Zattera, R.M.C. Santana, *J. Reinf. Plast. Compos.* **35**, 628 (2016)
14. M.B. Agustin, F. Nakatsubo, H. Yano, *Cellulose* **23**, 451 (2016)
15. K.Y. Lee, Y. Aitomaki, L.A. Berglund et al., *Compos. Sci. Technol.* **105**, 15 (2014)
16. I. Ugi, *Isonitrile Chemistry* (Academic, London, 1971)
17. R. Kaur, P. Kaur, S. Sharma, G. Singh, S. Mehndiratta, P.M.S. Bedi, K. Nepali, *Recent Pat. Anti-cancer Drug. Discov.* **10**, 23 (2015)
18. N.A. Al-Masoudi, Y.A. March, J.J. Al-Ameri, D.S. Ali, *Ch. Pannecouque, Chem. Biol. Inter.* **6**, 69 (2016)
19. W. Armarego, *The Chemistry of Heterocyclic Compounds; Fused Pyrimidines* (Wiley-Interscience, New York/London, 2009)
20. J.H. Lister, *The Chemistry of Heterocyclic Compounds; Fused Pyrimidines; In The Purines* (Wiley-Interscience, New York/London, 2009)
21. D.J. Brown, *The Chemistry of Heterocyclic Compounds In The Pyrimidines*, vol. 52 (Wiley-Interscience, New York, 2009)
22. A. Oliva, G. Zimmermann, H. W. Krell, *International Patent WO 98/58925* (1998)
23. J.P. De La Cruz, T. Carrasco, G. Ortega, F.S. De La Cousta, *Lipids* **27**, 192 (1992)
24. Y.S. Sanghvi, S.B. Larson, S.S. Matsumoto, *J. Med. Chem.* **32**, 629 (1989)
25. R.B. Tenser, A. Gaydos, K.A. Hay, *Antimicrob. Agents Chemother.* **45**, 3657 (2001)
26. A. Khalafi-Nezhad, F. Panahi, *Synthesis* **6**, 0984 (2011)
27. S.C. Jadhvar, H.M. Kasraliker, S.V. Goswami, S.R. Bhusare, *World J. Pharm. Pharm. Sci.* **4**, 1106 (2016)
28. B. Sadeghi, M.H. Sowlat Tafti, *J. Iran. Chem. Soc.* **13**, 1375 (2016)
29. H. Yousefi, M. Mashkour, R. Yousefi, *Cellulose* **22**, 1189 (2015)
30. H. Yousefi, S. Hejazi, M. Mousavi, Y. Azusa, A.H. Heidari, *Ind. Crops Prod.* **43**, 732 (2013)
31. B. Liu, Z. Zhang, K. Huang, *Cellulose* **20**, 2081 (2013)
32. K.M. Hello, H.R. Hasan, M.H. Sauodi, *Appl. Catal. A* **475**, 226 (2014)
33. K.-Y. Lee, T. Tammelin, K. Schulfter, H. Kiiskinen, J. Samela, A. Bismarck, *ACS Appl. Mater. Interface* **4**, 4078 (2012)